Cancer Science

WILEY

Cancer Science

ORIGINAL ARTICLE OPEN ACCESS

Variation of Gene Expression and Methylation Profiling in Gingival and Tongue Cancers

Takafumi Kashiwagi[1,2] | So Takata[1] | Hidenori Tanaka[1,3] | Shoko Ikuta[1] | Yasushi Totoki[1] | Yoichiro Nakatani[1,4] | Hidenori Inohara[3] | Narikazu Uzawa[2] | Shinichi Yachida[1]

[1]Department of Cancer Genome Informatics, Graduate School of Medicine, Osaka University, Suita, Osaka, Japan | [2]Department of Oral & Maxillofacial Oncology and Surgery, Graduate School of Dentistry, Osaka University, Suita, Osaka, Japan | [3]Department of Otorhinolaryngology-Head and Neck Surgery, Graduate School of Medicine, Osaka University, Suita, Osaka, Japan | [4]Laboratory of Medical and Evolutionary Genomics, Department of Biological Informatics, Bioinformatics Center, Research Institute for Microbial Diseases, Osaka University, Suita, Osaka, Japan

Correspondence: Narikazu Uzawa (uzawa.narikazu.dent@osaka-u.ac.jp) | Shinichi Yachida (syachida@cgi.med.osaka-u.ac.jp)

Received: 29 March 2025 | **Revised:** 9 September 2025 | **Accepted:** 12 September 2025

Funding: This work was supported by grants from Practical Research for Innovative Cancer Control from the Japan Agency for Medical Research and Development (AMED; JP22ck0106546 to S.Y.; JP23ck0106799 to S.Y.); Project for Cancer Research and Therapeutic Evolution from AMED (JP21cm0106477 to S.Y.); Project for Promotion of Cancer Research and Therapeutic Evolution from AMED (JP23ama221404 to S.Y.; JP24ama221430 to S.Y.); United States–Japan Cooperative Medical Science Program from AMED (JP23jk0210009 to S.Y.); JSPS KAKENHI (20H03662 to S.Y.; 23H02892 to S.Y.); JST-AIP Acceleration Research (JPMKCR19U3 to S.Y.); Integrated Frontier Research for Medical Science Division, Institute for Open and Transdisciplinary Research Initiatives, Osaka University (to S.Y.); the Takeda Science Foundation (to S.Y.); the Yasuda Medical Foundation (to S.Y.); the Mitsubishi Foundation (to S.Y.); the Princess Takamatsu Cancer Research Fund (to S.Y.);and Yakult Bio-Science Foundation (to S.Y.).

Keywords: DNA methylation | gene expression | immune profile analysis | intertumor heterogeneity | oral subsites

ABSTRACT

While the development of innovative drugs has improved the outcomes of various cancers in recent years, the number of patients with oral squamous cell carcinoma (OSCC) and mortality rates has not yet decreased significantly. This could be attributed to the prognostic and molecular differences occurring at different locations of cancer development. In this study, we conducted gene expression, DNA methylation, and tumor immunological analyses of gingival squamous cell carcinoma (GSCC) and tongue squamous cell carcinoma (TSCC) to elucidate the characteristic gene expression changes, their mechanisms, and tumor immune profiles. Gene expression analysis suggested that pathways related to the cell cycle and antibacterial humoral immunity were upregulated in GSCC, whereas immune response pathways were upregulated in TSCC. Additionally, high *HOXC13* expression may be associated with GSCC prognosis. DNA methylation analysis revealed hypermethylation of the 3′ UTR of the *HOXD11* gene, leading to increased expression in both GSCC and TSCC. In the tumor immune profile analysis, when comparing tumor and normal tissues in GSCC, the number of immune cells did not change significantly; however, the proportion of inflammatory cells, such as CD8+ T cells, changed. In TSCC, the number and percentage of inflammatory cells, such as T lymphocytes, increased in the tumor compared to those of normal tissues. These findings underscore the importance of understanding the characteristics of site-specific OSCC. Therefore, it is essential to establish standardized treatment protocols and develop novel therapeutic strategies tailored to each anatomical site of the tumor.

Abbreviations: GSCC, gingival squamous cell carcinoma; HNSCC, head and neck squamous cell carcinoma; *HOXC13-AS*, the antisense RNA of *HOXC13*; IL-1α, interleukin-1α; OSCC, oral squamous cell carcinoma; TCGA, the Cancer Genome Atlas; TSCC, tongue squamous cell carcinoma.

1 | Introduction

Oral squamous cell carcinoma (OSCC) is a type of cancer that constitutes head and neck squamous cell carcinoma (HNSCC). In 2018, approximately 350,000 new OSCC cases and 170,000 OSCC-related deaths were reported worldwide. Currently, the number of cases and mortality has not decreased significantly [1–3]. In addition to anticancer drugs, molecularly targeted drugs and immune checkpoint inhibitors have been introduced; however, their options remain limited. Therefore, the identification of new biomarkers and development of new treatments for OSCC are important issues [4]. One of the reasons for this is believed to be the heterogeneity of cancer cells and tumor microenvironment, which is composed of various immune cells within the same tumor or in the sublocation of the tumor origin.

Previous reports have shown that the prognosis differs for each subtype of OSCC [5, 6], with hard palate OSCC and gingival squamous cell carcinoma (GSCC) showing the worst prognosis. Molar OSCC, a type of GSCC, is the most common recurrence, followed by tongue squamous cell carcinoma (TSCC) [5], highlighting the importance of analysis and treatment of GSCC. In HNSCC, genetic mutations and the proportion of tumor-infiltrating lymphocytes, such as those in the larynx, pharynx, and tonsils, depend on the anatomical location of OSCC and non-OSCC HNSCC. It has also been reported that OSCC has more genetic mutations in *FAT1*, *CASP8*, *CDKN2A*, *NOTCH1*, and *PIK3CA* genes than in non-OSCC HNSCC [4]. In OSCC, buccal mucosa and tongue cancers were compared immunohistochemically for the expression of key cell cycle regulatory proteins to determine whether differences exist in the cell cycle regulatory mechanisms of these tumors, and significant differences in p16 and p21 expression were found [7].

However, in a comprehensive genomic analysis of HNSCC by the Cancer Genome Atlas (TCGA) Network [8], the study of OSCC has focused mainly on TSCC, and there have been few reports on the genomic analysis of OSCC other than TSCC, especially on GSCC. Epigenetic abnormalities occur during the early stages of carcinogenesis, and these changes are triggered by various factors. For instance, external factors such as alcohol consumption, smoking, and diet reportedly modulate epigenetic changes [9]. Periodontitis, which is caused by oral bacteria, induces epigenetic changes [10, 11]. These changes may affect the immune system. To the best of our knowledge, there have been no studies on comprehensive gene expression and methylation analyses or immune cell profile analyses comparing OSCC, which differs in its cell of origin, carcinogenic factors, and microenvironments with different anatomical sublocations.

In this study, we conducted transcriptomic, epigenomic, and tumor immunological analyses of GSCC, which is associated with poor prognosis and is the second most frequent OSCC next to TSCC in Japan. We also analyzed TSCC, which is relatively common among OSCC cases, to elucidate the characteristic changes in gene expression, underlying mechanisms, and tumor immune profiles in both the GSCC and TSCC subtypes. These findings may contribute to improved stratification and the development of therapeutic strategies for OSCC management.

2 | Materials and Methods

2.1 | Ethical Approval

This study was reviewed and approved by the Osaka University Research Ethics Review Committee (approval number: 768,937 [L001]). Study participants could opt out at any time, and the opportunity to deny participation was guaranteed.

2.2 | Study Participants and Tissue Samples

The study included 31 cases of gingival cancer and 27 cases of tongue cancer from patients diagnosed and operated on between January 2018 and November 2022 at the Department of Oral & Maxillofacial Oncology and Surgery, Osaka University Graduate School of Dentistry, and the Department of Otorhinolaryngology-Head and Neck Surgery, Osaka University Graduate School of Medicine.

Tissue samples were collected from surgical specimens in 5-mm squares from tumor and normal areas (gingival cases were included if 5-mm squares of tissue could be collected) and frozen at −80°C to the extent that postoperative pathology diagnosis was not affected.

2.3 | DNA and RNA Extraction and Quantitative and Qualitative Measurements

DNA and RNA were extracted from frozen tissue samples using the AllPrep DNA/RNA Mini Kit (Qiagen, Hilden, Germany) for frozen tumor tissues. The QIAamp DNA Mini Kit (Qiagen, Hilden, Germany) was used to extract DNA from normal frozen tissues, and RNA was extracted using an AllPrep DNA/RNA Mini Kit (Qiagen, Hilden, Germany).

DNA was analyzed using a NanoDrop One microspectrophotometer (Thermo Fisher Scientific, Waltham, Massachusetts, USA) and Qubit 2.0 Fluorometer (Invitrogen, Carlsbad, California, USA), a nucleic acid and protein quantification device. The 4200 TapeStation (Agilent Technologies, Santa Clara, California, USA) was used to quantify and measure the quality of RNA.

2.4 | Whole Transcriptome Analysis (RNA-Sequencing [RNA-Seq] Analysis)

The number of analyzed tumor cases was 31 gingival cases (tumor: 31, normal: 21), and 27 tongue cases (tumor: 27, normal: 15) were included. Total transcriptome sequencing libraries were prepared using Illumina Stranded Total RNA Prep (Illumina, San Diego, CA, USA). Sequencing was performed with 100 bp paired reads on a NovaSeq6000 and Transcripts Per Million (TPM) were calculated for each gene to determine gene expression.

The edgeR package [12] was used for the gene expression analysis of the two groups. Differences in gene expression were

determined using the likelihood ratio test, with the value of |logFC| used to assess the magnitude of expression and p-value used to assess statistically significant differences. Genes with |log2FC| > 1 and $p < 0.05$ were excluded from the screening.

2.5 | Enrichment Analysis

Enrichment analysis was performed using Metascape (https://www.metascape.com), which is based on over 40 datasets across 10 model organisms (human, mouse, and rat) and is functional. It is an analysis tool that performs a combination of functions, such as enrichment analysis, interactome analysis, gene annotation search, and refinement of data that meet certain criteria, such as specific Gene Ontology (GO) terms [13]. The expression variation genes identified using the likelihood ratio test were listed, a text file was created and uploaded to the Metascape website, and the associated pathways were identified and analyzed.

2.6 | Assessment of Prognostic Information

In this study, patients with postoperative recurrence of the primary tumor or neck and iatrogenic cervical lymph node metastases were classified into the recurrent/metastatic group. Cases wherein prognostic information was difficult to obtain due to death or transfer to another hospital were terminated when their progress could not be followed up.

2.7 | Survival Prognostic Analysis

Survival prognostic analysis was performed using the Kaplan–Meier method with the Survminer package (https://github.com/kassambara/survminer) to verify differences in survival prognosis among patient groups with different gene expression levels and clusters.

2.8 | DNA Methylation Array Analysis

The number of analyzed cases was 30 gingival cases (30 tumor and 7 normal samples) and 27 tongue cases (27 tumor and 7 normal samples). A comprehensive DNA methylation array analysis was performed using the Infinium MethylationEPIC BeadChip Kit (Illumina, San Diego, California, USA), and methylation levels at CpG sites were expressed as beta values ranging from 0 (not fully methylated) to 1 (fully methylated). The R package ChAMP pipeline (version 2.18.2) was used for data quality control, preprocessing, normalization, and the detection of differentially methylated regions (DMRs) [14]. To remove the influence of age-related epigenetic abnormalities, we performed a linear regression of age for each CpG on the β values and corrected them using the residuals and mean. BMIQ was used for normalization, and ProbeLasso was applied to define DMRs with the following parameters: minProbes = 3, meanLassoRadius = 1200, adjPvalDmr = 0.05, and cores = 3.

2.9 | Tumor Immune Profiling Analysis Using Whole Transcriptome Data

The expression profiles of each cell type of interest (22 tumor immune cell types) were assessed and examined by subsite and tumor site-to-normal sites using the CIBERSORTx method [15], a digital flow cytometric method for analyzing tumor immune environments from bulk RNA-seq data. Tximport TPM data were used, where the expression levels per transcript (RNA components, such as genes and exons) were aggregated and organized in a uniform format in TPM data that were uploaded to the official CIBERSORTx website (CIBERSORTx (stanford.edu)). Samples with $p < 0.05$ were excluded, but none were found in this study.

Furthermore, an Immunogram [16, 17] was used. This tool analyzes and scores the entire system from multiple and composite angles and refers to the immune response. ssGSEA functions were set up, and scores were calculated using R software (v4.2.0) (https://www.r-project.org). A list of genes for each item (axis) was created, and a heatmap was generated.

2.10 | Statistical Analysis

All statistical analyses were performed using R software (v4.0.2) and Microsoft Excel (v16.79.1) (One Microsoft Way, Redmond, Washington, USA). Patient survival was analyzed using the Kaplan–Meier method in the survival package, and the significance of the differences between survival curves was determined using the log-rank test.

Owing to the low area under the receiver operating characteristic (ROC) curve (AUC), the cutoff value for tongue cancer was determined by dichotomizing the data at the median. In contrast, for gingival cancer, the cutoff value was established through ROC curve analysis (AUC = 0.707), and the optimal threshold was identified using the Youden index, yielding a cutoff value of 7.35 (Figure S4B). Accordingly, the cutoff value for gingival cancer was rounded to 7.

3 | Results

3.1 | Study Population

In total, 31 patients with GSCC and 27 patients with TSCC were included in this study. The clinicopathological characteristics of the study population are presented in Table 1. When comparing GSCC and TSCC cases, the median age of patients with GSCC was significantly higher ($p = 0.0004$), and there were more women with GSCC and more men with TSCC. Additionally, TSCC was more closely associated with a history of alcohol consumption than gingival cancer ($p = 0.0076$). No significant differences were noted between GSCC and TSCC regarding the presence or absence of lymph node metastasis (pN classification, $p = 0.6261$); however, in terms of the size of the primary tumor (pT classification), there were more advanced cases of GSCC than TSCC ($p = 0.0226$).

TABLE 1 | Information on the clinicopathological characteristics of gingival squamous cell carcinoma (GSCC) and tongue squamous cell carcinoma (TSCC) in this study.

	GSCC	TSCC	
	N **= 31**	***N*** **= 27**	***p***
Sex			
Male	13	16	0.3789
Female	18	11	
Age			
Median	77	66	0.0004
Range	50–89	30–89	
Smoking history			
10 pack-years	15	11	0.4000
≥ 10 pack-years	8	10	
Unknown	8	6	
Alcohol history			
Non-drinker	14	4	0.0076
Drinker	9	15	
Unknown	8	8	
p T classification[a]			
T1	5	7	0.0226
T2	7	9	
T3	1	7	
T4	17	4	
Unknown	1	0	
p N classification[a]			
N0	24	20	0.6261
N1	3	0	
N2	0	7	
N3	3	0	
Unknown	1	0	
p stage			
I	5	7	0.1445
II	7	8	
III	1	3	
IV	17	9	
Unknown	1	0	

[a]*p T, N classification*: Compliant with the 8th edition of the UICC TNM classification system.

We examined the prognosis of GSCC and TSCC. Figure S1A,B shows the results of Kaplan–Meier analysis of GSCC and TSCC divided into early-stage (p Stage I/II) and advanced-stage (p Stage III/IV) cases, respectively. Contrary to previous reports [5], we confirmed that in early-stage cases, TSCC had a worse prognosis than GSCC. However, in advanced-stage cases, there was little significant difference in prognosis. We also divided the GSCC and TSCC cases into lymph node metastasis-positive and -negative groups and analyzed the prognosis of each group (Figure S2A,B). No clear differences in prognosis were observed between GSCC and TSCC, regardless of whether lymph node metastasis was positive or negative.

3.2 | Gene Expression Analyses Across GSCC and TSCC

First, gene expression analysis was performed to identify gene clusters with greater changes in gene expression in whole GSCC and TSCC than in normal samples. *HOX* and *MMP* genes were identified as gene clusters with large changes in expression, as shown in the heatmap (Figure 1A). Certain *HOX* genes, such as *HOXC11*, were compared separately between the tongue and gingiva. These results showed that the expression in the tumor increased compared to that of normal samples in both gingiva and tongue, but the expression status of each *HOX* gene differed between tongue and gingiva depending on each *HOX* gene (Figure 1B).

Next, we selected genes with a high tumor/normal gene expression ratio in GSCC and TSCC and created a heatmap based on these genes, resulting in clustering of GSCC and TSCC (Figure 1C). Therefore, we considered it necessary to perform clustering separately for the gingival and tongue cases.

3.3 | Gene Expression Analyses Between Each Normal and Cancer Sample From GSCC and TSCC

We performed gene expression and enrichment analyses between normal and cancer samples from GSCC and TSCC cases to confirm their gene expression and pathways. Figure 2A shows a volcano plot of the gene expression analysis in normal samples. The expression of *PIGR*, *IRX1*, and *MUC5B* increased in the gingiva, whereas the expression of *SBK2, HOXA3*, and *LRRC24* increased in the tongue. The gingival results showed that gene clusters that were upregulated in normal tissues were strongly associated with pathways in response to immunity, inflammation, and bacteria (Figure 2B). However, in the tongue, the upregulated gene clusters were strongly associated with pathways related to anatomical structures such as muscles (Figure 2C). Furthermore, when cancer tissues were compared, the tissue-specific gene clusters identified in the normal tissue comparison analysis were confirmed at each site. The expression of *FDCSP*, *MIA*, and *RPL36A* was increased (Figure 2D), and a "Neutrophil degranulation" cluster was identified in the gingival cancer tissue (Figure 2E). In tongue cancer tissue, the expression of *ACTA1*, *MYH2*, and *COX6A2* was increased (Figure 2D), and several of the same top clusters, such as "muscle structure development" and "muscle system process," were observed (Figure 2F). Thus, we considered the tumor/normal gene expression ratio, discovering that in the gingival cases, the expression of *MAGEA3*, *MAGEA4*, and *MMP1* was increased in cancer tissue (Figure S3A), and cell cycle clusters were upregulated (Figure S3B). In tongue cases, the expression of *CST1*, *MAGEA3*, and *MAGEA6* was increased in cancer tissue (Figure S3C), and cell activation and immune clusters were upregulated (Figure S3D).

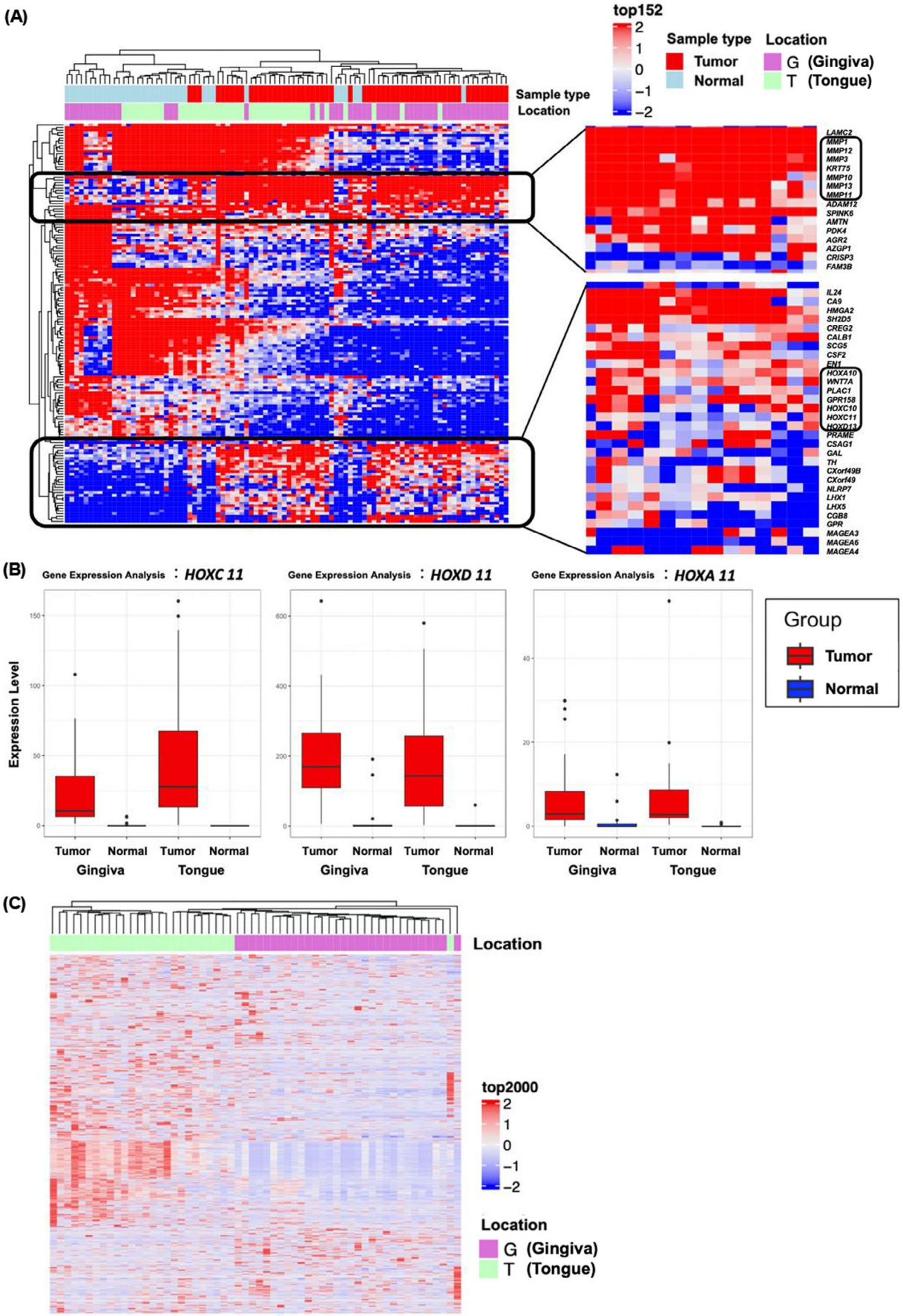

FIGURE 1 | Legend on next page.

FIGURE 1 | Gene expression analysis of GSCC and TSCC and clustering analysis using heat maps of genes with high variance. (A) Heatmap of gene expression analysis of GSCC and TSCC compared to that of the normal samples. (B) Analysis of *HOXC11*, *HOXD11*, and *HOXA11* expression by sublocation. (C) In GSCC and TSCC, the top 2000 genes with high variance in the tumor/normal area ratio were selected, and a heatmap was created, resulting in separate clustering for GSCC and TSCC.

3.4 | Gene Expression Analysis by Sublocations for Gingival and Tongue Cancer

In the analysis performed for GSCC and TSCC, we selected the top 2000 genes with a high tumor/normal gene expression ratio and created a heatmap. No obvious clustering was observed in GSCC, and no significant difference was observed in the Kaplan–Meier analysis (Figure 3A). We performed the same analysis in TSCC, which was clustered (Figure 3B), and a trend was observed in the Kaplan–Meier analysis of clusters 1 and 2 ($p=0.055$), suggesting a possible influence on recurrence and metastasis (Figure 3B). The clinicopathological characteristics of clusters 1 and 2 in GSCC and TSCC, respectively, are summarized in Tables S1 and S2. Next, we analyzed gene expression in the recurrent/metastatic and nonrecurrent/metastatic groups of TSCC, demonstrating that the expression of *CXCL* and immune system genes was significantly increased in the nonrecurrent/metastatic group, suggesting that these gene clusters are related (Figure 3C). In addition, enrichment analysis showed that the significantly upregulated genes in the nonrecurrent/metastatic group were strongly associated with acquired immune and inflammatory response pathways (Figure 3D). Furthermore, we observed a trend toward a low immune response (cold tumor) in the recurrent/metastasis group (cluster 2) and high immune response (hot tumor) in the nonrecurrent/metastasis group (cluster 1) using immunograms [16, 17] (Figure 3E).

3.5 | Comparison of Sublocations of GSCC and TSCC

We compared the gene expression and enrichment analyses of GSCC and TSCC in terms of tumor/normal expression ratios. Gene expression of the immune system was enhanced in TSCC compared to that in GSCC and was strongly associated with immune response pathways (Figure 4A,B). Interleukin-1α (IL-1α) is known to function as a potent mediator of oral bacterial and microbial invasion [18]. We observed that *IL1A* expression was markedly enhanced in GSCC compared with that in TSCC. In addition, genes related to the antimicrobial humoral immune response pathway induced by antimicrobial peptides, such as *DEFB103A* and *DEFB4A*, including *IL1A*, were expressed at higher levels (Figure 4A,C). The cell cycle was the most activated pathway identified. *HOXC13* and *HOXA6*, members of the *HOX* gene family, were also upregulated (Figure 4A). These results identified *IL1A* as a characteristic gene of GSCC compared with that of TSCC, suggesting a strong involvement of the cell cycle and oral bacteria in the development of GSCC. Moreover, *HOXC13*, a *HOX* gene whose expression is upregulated in OSCC, was identified. We considered the association between the expression ratio of *HOXC13* and GSCC prognosis. First, we calculated the cutoff value of the receiver operating characteristic curve (cutoff value = 7.35, AUC = 0.707) using the Youden index (Figure S4B) and approximated it to an integer value. We performed Kaplan–Meier analysis and divided the expression ratio of *HOXC13* in GSCC into two at 7.0 and observed a significant difference in disease-free survival calculated using the log-rank test ($p=0.033$, Figure 4D). The clinicopathological characteristics of GSCC according to the *HOXC13* expression ratio (tumor/normal) ≥ 7.0 or < 7.0 are listed in Table S3.

3.6 | DNA Methylation Array Analysis Using DNA Methylation Data

DNA methylation array analysis was performed to investigate whether epigenomic aberrations altered the expression of *HOX* and other genes with upregulated expression in GSCC and TSCC. Gene expression is generally suppressed by methylation of the promoter regions and enhanced by demethylation of them [19].

First, we examined the relationship between gene expression and methylation of the promoter regions in the whole GSCC and TSCC. The promoter regions were methylated rather than demethylated for some *HOX* genes, and their expression was upregulated (Figure 5A).

HOXD11 was upregulated after methylation of the 3′ UTR in both TSCC and GSCC (Figure 5B–D). We observed correlations between gene expression levels and methylation of the 3′ UTR is (Figure S5), and a slight correlation was observed for *HOXD11* (Figure S5).

3.7 | Comparison and Examination of Immune Cell Infiltration in Sublocations and Between Tumor and Normal Samples

Using CIBERSORTx [15], we compared and examined immune cell infiltration between normal areas of the gingiva and tongue as well as between the tumor and normal areas for each sublocation using the expression profiles of 22 cell types.

A comparison between normal sections of the gingiva and tongue showed that the number and percentage of tumor immune cells of each of the 22 cell types differed between locations, with the gingiva showing a higher overall number of immune cells (Figure 6A). The number of immune cells did not change significantly when comparing tumor and normal areas in GSCC; however, the proportion of inflammatory cells changed, including CD8+ T cells (Figure 6B). In each of the 22 cell types, there were significant differences in the number of eight immune cells and five immune cells: activated dendritic cells, eosinophils, M0 macrophages, CD4 memory-activated T cells, and CD4 naïve T cells. These cells were significantly increased in the tumor-specific sections. The absolute numbers of three immune cell types, naïve B cells, activated mast cells, and CD4 memory resting T cells, decreased in the tumor-specific parts (Figure S6A,D). In TSCC, the number and percentage

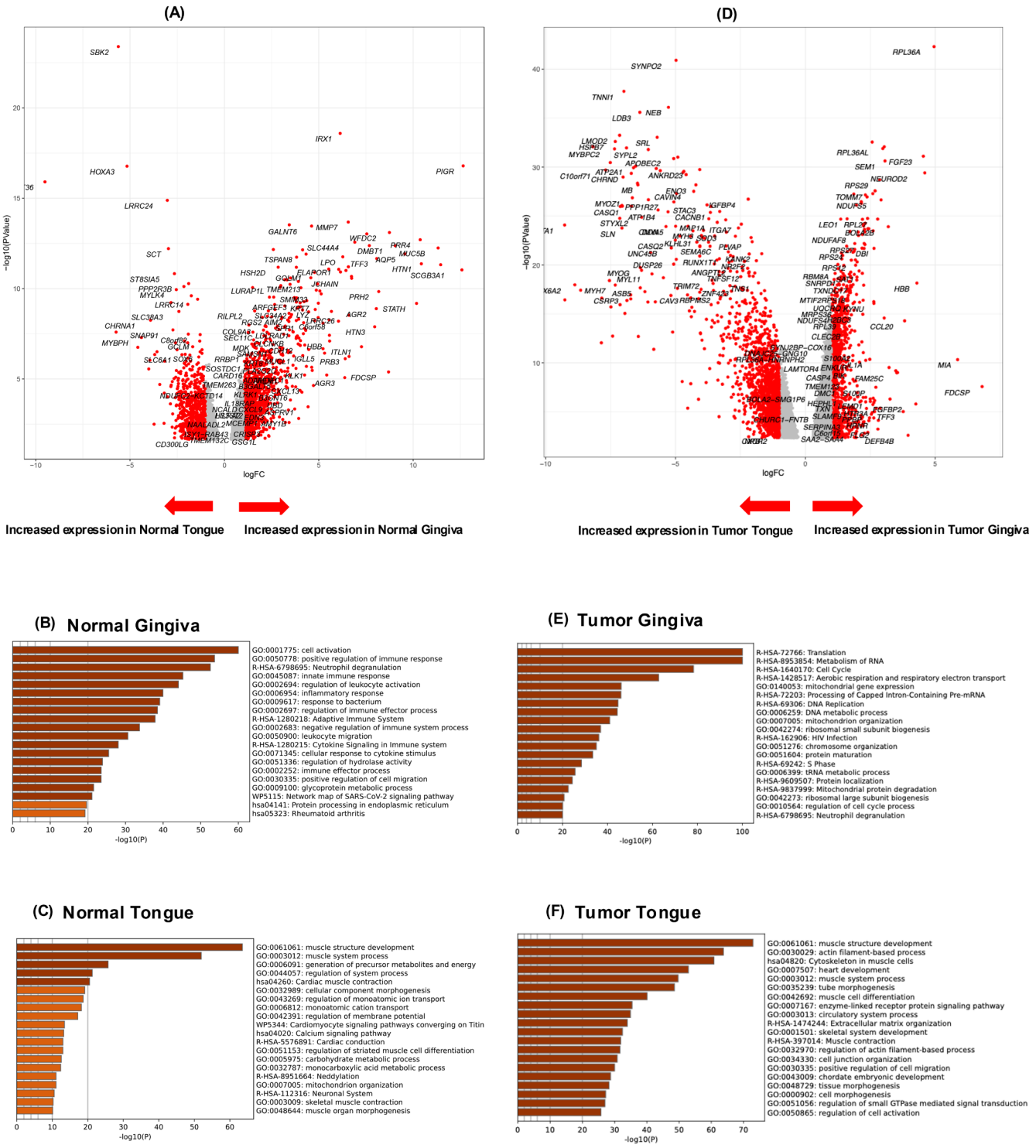

FIGURE 2 | Results of gene expression and enrichment analyses using genes observed in normal tissues in each area. (A) Volcano plot indicating gene expression in normal gingival and tongue areas. An absolute value of log fold change (|logFC|) > 1 and $p < 0.05$ were used as cutoffs. (B) Characteristic pathways in normal tissues in the gingiva. Gene expression and pathways related to immunity, inflammation, and bacteria were also observed in the normal tissues. (C) Characteristic pathways in normal tissues in the tongue. Gene expression and pathways related to anatomical structures were also observed. (D) Volcano plot indicating gene expression in the gingival and tongue tumor areas. An absolute value of |logFC| > 1 and $p < 0.05$ were used as cutoffs. (E) Characteristic pathways in tumor tissues of the gingiva. Neutrophil degranulation and cell cycle clusters were identified in the gingival cancer tissue. (F) Characteristic pathways in tumor tissues in the tongue. Gene expression and pathways related to anatomical structures were observed like normal tissues.

of inflammatory cells, such as T lymphocytes, increased in the tumor compared to those of normal tissues (Figure 6C). Significant differences were also observed between certain immune cell types. The absolute numbers of regulatory T cells (Tregs), naïve B cells, activated dendritic cells, M0 macrophages, M1 macrophages, plasma cells, CD4 memory-activated T cells, resting CD4 memory T cells, and CD8 T cells were increased in the tumor, whereas the absolute numbers of eosinophils and monocytes decreased in the tumor (Figure S6B,E).

Prognostic analysis of each of the 22 tumor immune cell types for each GSCC and TSCC sublocation was performed using the log-rank test, and no significant differences were observed for any of the immune cell types.

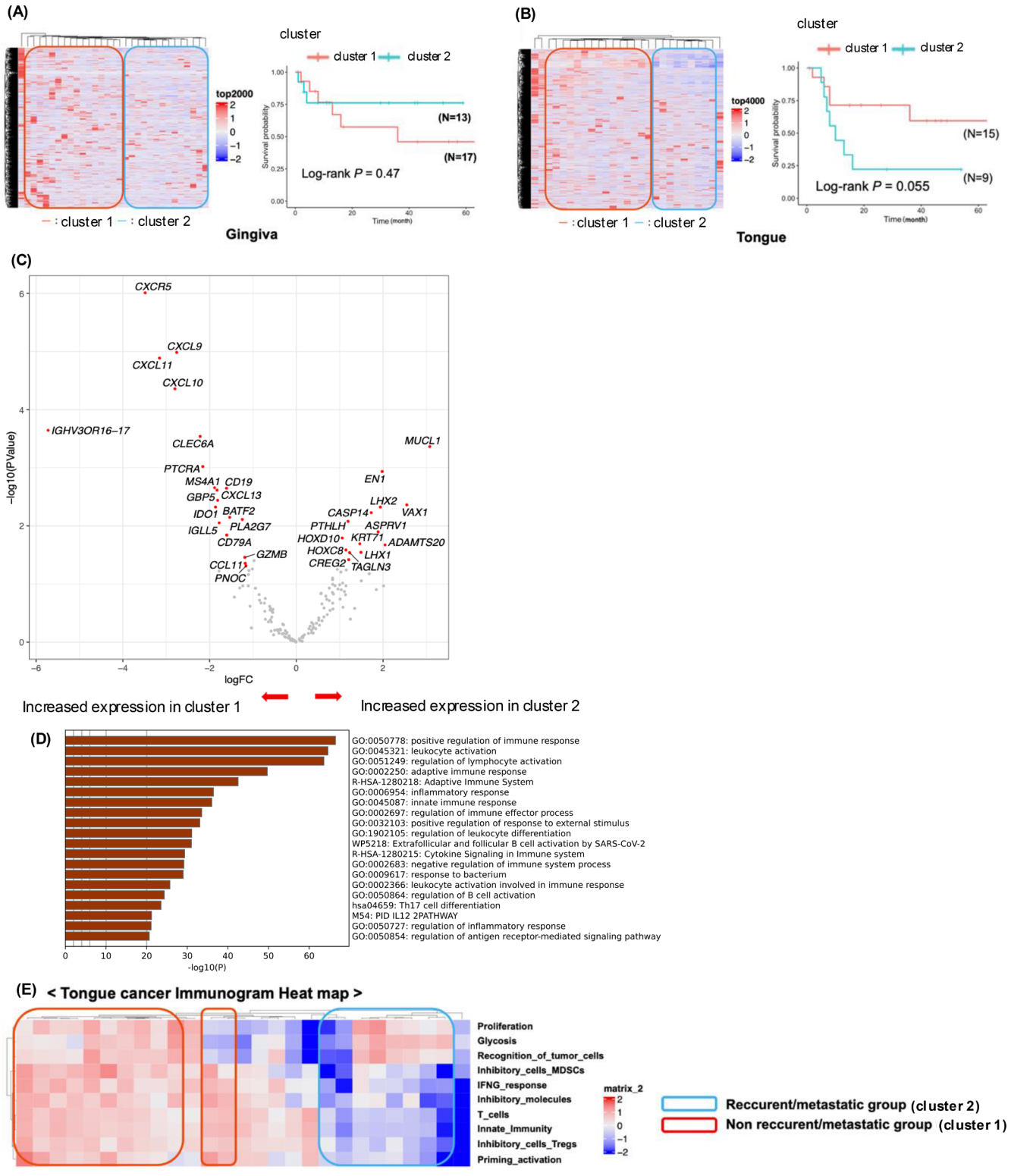

FIGURE 3 | Legend on next page.

FIGURE 3 | Gene expression analysis by sublocations for GSCC and TSCC. (A) In GSCC, genes with high variance in the tumor/normal ratio were selected, and a heatmap was created. Clustering analysis was performed; however, no clear clustering was observed. Furthermore, Kaplan–Meier analysis was performed to examine the association with prognosis for each cluster, but no significant differences were observed. (B) In TSCC, genes with high variance in the tumor/normal ratio were selected, and a heatmap was created. Clustering analysis was performed, and the genes were roughly clustered into two groups, which were named clusters 1 and 2. In clusters 1 and 2, Kaplan–Meier analysis was performed to examine the association with prognosis. (C) Volcano plot showing the results of gene expression analysis in the recurrent/metastatic group (cluster 2) and non-recurrent/metastatic group (cluster 1) of tongue cancer cases. *CXCL* genes and immune system genes were involved in the nonrecurrent/metastatic group (cluster 1). An absolute value of $|\log FC| > 1$ and $p < 0.05$ were used as cutoffs. (D) Enrichment analysis was performed between the two groups (C), and pathways characteristic of the nonrecurrent/metastatic group (cluster 1) are shown. Gene expression and pathways related to acquired immunity and inflammation were also observed. (E) A heatmap was created for the immunogram, highlighting tongue cancer cases. The red areas in the heatmap indicate a high immune response (hot tumor), and the blue areas indicate a low immune response (cold tumor).

4 | Discussion

In this study, gene expression analysis revealed that genes that were significantly upregulated in normal gingiva were strongly related to immune, inflammatory, and bacterial response pathways and that pathways related to the cell cycle and antibacterial humoral immunity were upregulated in GSCC. Genes related to anatomical pathways, such as muscle development, were upregulated in normal tongue samples, and immune response pathways were upregulated in TSCC. In addition, the high expression of *HOXC13* may be associated with the GSCC prognosis. DNA methylation analysis showed that *HOXD11* gene expression was increased by hypermethylation of the 3′ UTR. In the tumor immune profile analysis, when comparing tumor and normal tissues in GSCC, the number of immune cells did not change significantly, but the proportion of inflammatory cells, such as CD8+ T cells, changed. Furthermore, the prognosis of early-stage TSCC was worse than that of GSCC in this study.

Similar to previous reports on the observed prognoses of GSCC and TSCC, we expected the prognosis of GSCC to be worse than that of TSCC. However, the study results were different from our expectations, and this discrepancy may be attributed to prior studies that conducted analyses based solely on tumor location without accounting for other factors such as disease stage or sample size. Currently, there are no well-established standard treatments or surgical procedures specific to gingival cancer. Surgical intervention for both cancer types is generally undertaken to achieve curative resection. In tongue and gingival cancers, prophylactic neck dissection was performed only when the primary tumor was large, oral resection was technically challenging, or reconstructive procedures were required. Alcohol consumption is known to be one of the risk factors for OSCC [20] and may be related to TSCC among OSCC.

HOX genes have been reported to act as tumor suppressors; however, they have also been reported to contribute to oncogenesis in various cancer types, and the *HOX* genes that may cause oncogenesis differ for each cancer type [21, 22]. Kanaka et al. reported that the expression of *HOXA7*, *HOXA10*, *HOXB7*, *HOXC6*, *HOXC10*, *HOXD10*, and *HOXD11* increased in OSCC and that posterior *HOX* genes were associated with carcinogenesis compared to that of anterior *HOX* genes [23]. Our results are similar to those of previous reports [23]. One of the major characteristics of the oral cavity, including the gingiva and tongue, is the presence of oral bacteria that cause caries, periodontal disease, and other diseases [24, 25]. In recent years, oral bacteria, including those that cause periodontal disease, have been reported to be involved in the carcinogenesis and progression of OSCC [26]. This may indicate that the gingiva is more susceptible to bacteria in oral plaque and mechanical stimuli due to chewing meals using dentures, etc., compared to the tongue [27]. This suggests that oral bacteria and inflammation against bacteria and bacterial toxins may be deeply involved in the development and progression of GSCC [28]. In TSCC, inflammation and changes in the immune system due to contact with teeth and other factors may be involved in carcinogenesis and progression [29]. *HOXC13* is highly expressed in various cancer types [30, 31], and in breast cancer, high *HOXC13* expression has been associated with poor prognosis, tumor stage, and regional lymph node metastasis [32]. In OSCC, antisense RNA of *HOXC13* (*HOXC13-AS*) has been reported to increase *HOXC13* expression and promote cell growth and migration [33]. To date, there have been no reports that mention the possibility that *HOXC13* may be a prognostic factor in GSCC and other OSCC.

Although the possible mechanisms underlying DNA methylation in promoter regions and increased gene expression are currently unclear, several hypotheses have been reported [34]. Previous genomic analyses of several cancers have shown that DNA methylation in the 3′ UTR may be associated with increased gene expression [35]. Our results for *HOX* genes in GSCC and TSCC support these reports and suggest that methylation of promoter regions may enhance gene expression.

Regarding tumor immune profiling analysis, we hypothesized that the differences between the gingiva and tongue were due to the different anatomical structures and cells of origin in the same oral cavity. Yao et al. used data from 400 OSCC samples from TCGA database to assess immune cell infiltration using CIBERSORTx [36], similar to our results, and observed that the absolute numbers of M0 macrophages, activated dendritic cells, and CD4 memory-activated T cells were increased in tumors compared to that of normal areas. As TSCC constitutes the majority of OSCC in the TCGA database [8], a correlation with our results for TSCC was expected; however, no significant correlation was found. Differences in the number of cases, race of the case subjects, and external factors such as alcohol consumption and smoking may have influenced the results of the analyses.

The limitations of this study include the difficulty in collecting and analyzing tumor and normal tissue samples in pairs for all cases, considering the size of the lesion in the surgical

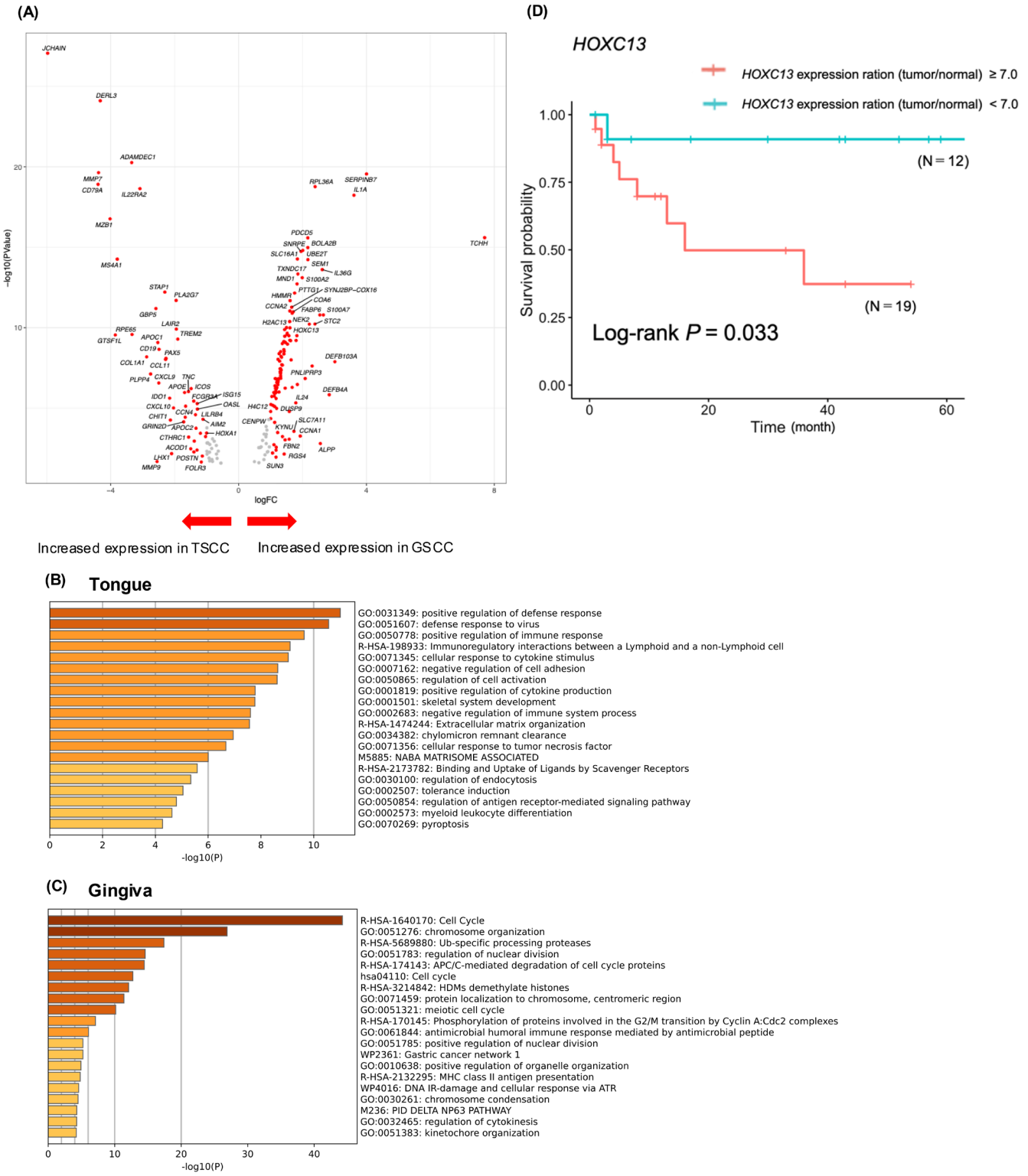

FIGURE 4 | Comparison of gingival and tongue cancer subsites. (A) The results of gene expression analysis of gingival and tongue cancer based on the tumor/normal ratio are shown in a volcano plot. An absolute value of $|\log FC| > 1$ and $p < 0.05$ were used as cutoffs. (B, C) Results of enrichment analysis between the GSCC and TSCC groups. (D) Kaplan–Meier curves were drawn based on disease-free survival rates for GSCC patients with *HOXC13* expression ratios (tumor/normal) of ≥ 7.0 (high) and < 7.0 (low).

specimen and its effect on postoperative histopathological diagnosis, limiting the number of cases analyzed. In addition, as most of the samples were surgical samples obtained within a few years, the postoperative follow-up period was short, and it was difficult to examine the 5-year survival rate. The ages of the study participants varied widely, and the analysis considering age in normal tissues was insufficient. Second, this study was conducted at a single institution; therefore, the number of cases was limited. Furthermore, in this study, normal tissues were obtained from areas adjacent to the tumor

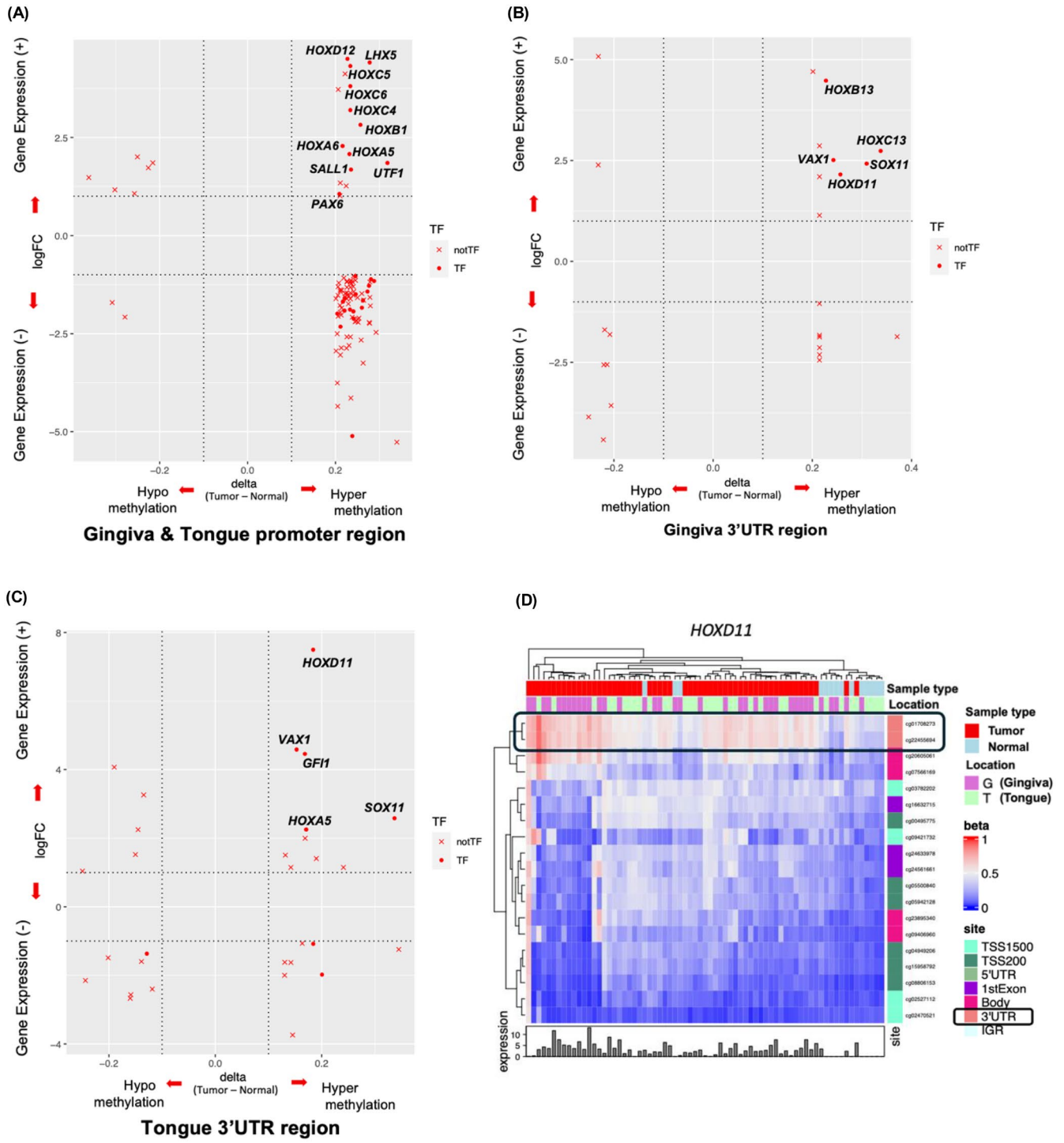

FIGURE 5 | Scatter plot and heatmap of β-delta and gene expression in DNA methylation array analysis. (A) Scatter plot showing the relationship between gene expression and promoter methylation in the two groups of tumor and normal areas of GSCC and TSCC. The horizontal axis delta indicates the difference in methylation, with methylation to the right of 0 and demethylation to the left. The vertical axis logFC above 0 indicates that gene expression increases in the tumor, whereas values below 0 are observed in the normal area. (B, C) Scatter plot showing the relationship between gene expression and methylation in the 3′ UTR in the two groups of tumor and normal areas of GSCC (B) and TSCC (C). (D) Heatmap showing the methylation and gene expression of *HOXD11*. TF, transcription factor.

resection sites. Such tissues may exhibit epigenetic abnormalities affecting the entire oral cavity, and ideally, samples from anatomically distant sites presumed to be entirely normal should be collected. Conversely, even tissues obtained from distant sites presumed to be normal may harbor epigenetic alterations as an acquired predisposing state. In future studies, we plan to collect both adjacent and distant normal tissue samples to enable a comprehensive comparison and further elucidate the presence and distribution of epigenetic abnormalities in normal tissue.

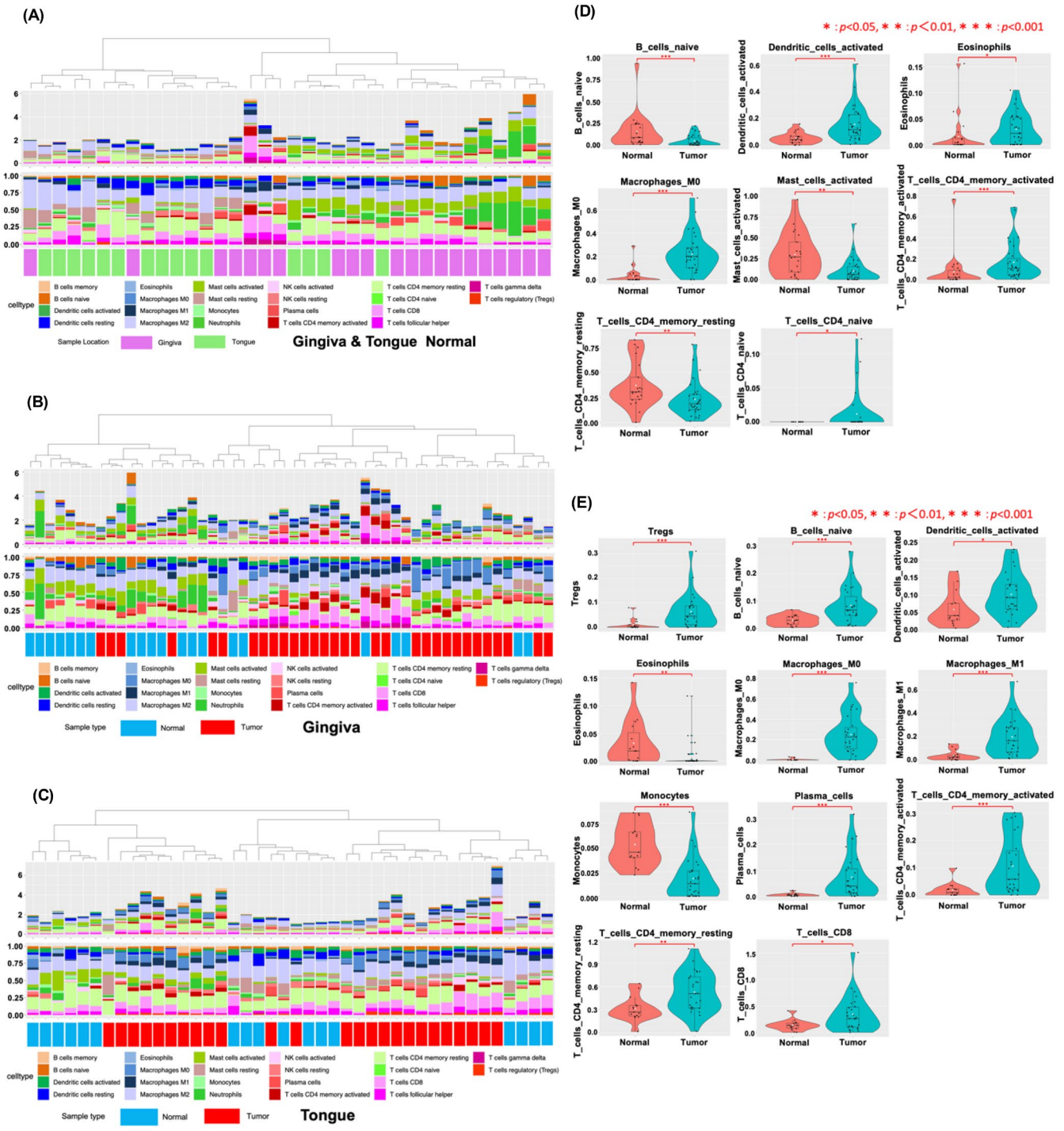

FIGURE 6 | Comparison and evaluation of tumor immune cell infiltration using CIBERSORTx analysis. (A) The horizontal axis shows the cases, and the vertical axis shows the number and ratio of tumor immune cells. When comparing the normal areas of the gingiva and tongue, the number and ratio of 22 types of tumor immune cells differ in each area, and the number of immune cells is higher in the gingiva. (B) Bar graph comparing tumor immune cells in the tumor and normal areas of the GSCC case. (C) Bar graph comparing tumor immune cells in the tumor and normal areas of the TSCC case. (D) Significant differences were observed in 8 of the violin plots comparing 22 types of immune cells in the tumor and normal areas of GSCC cases. (E) Significant differences were observed in 11 violin plots comparing 22 types of immune cells in the tumor and normal areas of TSCC cases.

Transcriptomic and epigenomic analyses revealed distinct gene alterations in normal and tumor tissues specific to each subsite. Therefore, it is evident that OSCC should not be regarded as a single disease entity but should instead be stratified by subsite. These results are expected to contribute to the establishment of standardized treatment protocols for postoperative recurrence and the development of novel therapeutic approaches tailored to each subsite.

Author Contributions

Takafumi Kashiwagi: data curation, formal analysis, investigation, methodology, resources, software, validation, visualization, writing – original draft, writing – review and editing. **So Takata:** formal analysis, software, validation, writing – review and editing. **Hidenori Tanaka:** resources, writing – review and editing. **Shoko Ikuta:** formal analysis, software, writing – review and editing. **Yasushi Totoki:** formal analysis, methodology, validation, writing – review and editing. **Yoichiro Nakatani:** formal analysis, writing – review and editing. **Hidenori Inohara:** resources, writing – review and editing. **Narikazu Uzawa:** conceptualization, methodology, project administration, resources, supervision, validation, writing – original draft, writing – review and editing. **Shinichi Yachida:** conceptualization, data curation, formal analysis, funding acquisition, methodology, project administration, supervision, validation, writing – original draft, writing – review and editing.

Ethics Statement

Approval of the research protocol by an Institutional Review Board: This study was reviewed and approved by the Osaka University Research Ethics Review Committee (approval number: 768,937 [L001]).

Consent

Informed consent was obtained from all study participants.

Conflicts of Interest

Shinichi Yachida is an Associate Editor of *Cancer Science*. The other authors have no conflicts of interest to declare.

References

1. H. Sung, J. Ferlay, R. L. Siegel, et al., "Global Cancer Statistics 2020: GLOBOCAN Estimates of Incidence and Mortality Worldwide for 36 Cancers in 185 Countries," *CA: A Cancer Journal for Clinicians* 71 (2021): 209–249, https://doi.org/10.3322/caac.21660.

2. S. Muller and W. M. Tilakaratne, "Update From the 5th Edition of the World Health Organization Classification of Head and Neck Tumors: Tumors of the Oral Cavity and Mobile Tongue," *Head and Neck Pathology* 16 (2022): 54–62, https://doi.org/10.1007/s12105-021-01402-9.

3. C. Harsha, K. Banik, H. L. Ang, et al., "Targeting AKT/mTOR in Oral Cancer: Mechanisms and Advances in Clinical Trials," *International Journal of Molecular Sciences* 21 (2020): 3285, https://doi.org/10.3390/ijms21093285.

4. A. W. Y. Chai, K. P. Lim, and S. C. Cheong, "Translational Genomics and Recent Advances in Oral Squamous Cell Carcinoma," *Seminars in Cancer Biology* 61 (2020): 71–83, https://doi.org/10.1016/j.semcancer.2019.09.011.

5. N. C. Lin, S. I. Hsien, J. T. Hsu, and M. Y. C. Chen, "Impact on Patients With Oral Squamous Cell Carcinoma in Different Anatomical Subsites: A Single-Center Study in Taiwan," *Science Reports* 11 (2021): 15446, https://doi.org/10.1038/s41598-021-95007-5.

6. M. M. Justesen, H. Stampe, K. K. Jakobsen, et al., "Impact of Tumor Subsite on Survival Outcomes in Oral Squamous Cell Carcinoma: A Retrospective Cohort Study From 2000 to 2019," *Oral Oncology* 149 (2024): 106684, https://doi.org/10.1016/j.oraloncology.2024.106684.

7. K. M. Sathyan, R. Sailasree, R. Jayasurya, et al., "Carcinoma of Tongue and the Buccal Mucosa Represent Different Biological Subentities of the Oral Carcinoma," *Journal of Cancer Research and Clinical Oncology* 132 (2006): 601–609, https://doi.org/10.1007/s00432-006-0111-y.

8. Cancer Genome Atlas Network, "Comprehensive Genomic Characterization of Head and Neck Squamous Cell Carcinomas," *Nature* 517 (2015): 576–582, https://doi.org/10.1038/nature14129.

9. S. B. Mali, "Epigenetics: Promising Journey So Far but Ways to Go in Head Neck Cancer," *Oral Oncology* 135 (2022): 106194, https://doi.org/10.1016/j.oraloncology.2022.106194.

10. G. M. Richter, J. Kruppa, H. G. Keceli, et al., "Epigenetic Adaptations of the Masticatory Mucosa to Periodontal Inflammation," *Clinical Epigenetics* 13 (2021): 203, https://doi.org/10.1186/s13148-021-01190-7.

11. D. C. Andia, A. C. Planello, D. Portinho, et al., "DNA Methylation Analysis of SOCS1, SOCS3, and LINE-1 in Microdissected Gingival Tissue," *Clinical Oral Investigations* 19 (2015): 2337–2344, https://doi.org/10.1007/s00784-015-1460-1.

12. Y. Chen, A. T. Lun, and G. K. Smyth, "From Reads to Genes to Pathways: Differential Expression Analysis of RNA-Seq Experiments Using Rsubread and the edgeR Quasi-Likelihood Pipeline," *F1000Research* 5 (2016): 1438, https://doi.org/10.12688/f1000research.8987.2.

13. Y. Zhou, B. Zhou, L. Pache, et al., "Metascape Provides a Biologist-Oriented Resource for the Analysis of Systems-Level Datasets," *Nature Communications* 10 (2019): 1523, https://doi.org/10.1038/s41467-019-09234-6.

14. Y. Tian, T. J. Morris, A. P. Webster, et al., "ChAMP: Updated. Methylation Analysis Pipeline for Illumina BeadChips," *Biodiversity Informatics* 33 (2017): 3982–3984, https://doi.org/10.1093/bioinformatics/btx513.

15. A. M. Newman, C. B. Steen, C. L. Liu, et al., "Determining Cell Type Abundance and Expression From Bulk Tissues With Digital Cytometry," *Nature Biotechnology* 37 (2019): 773–782, https://doi.org/10.1038/s41587-019-0114-2.

16. T. Karasaki, K. Nagayama, H. Kuwano, et al., "An Immunogram for the Cancer-Immunity Cycle: Towards Personalized Immunotherapy of Lung Cancer," *Journal of Thoracic Oncology* 12 (2017): 791–803, https://doi.org/10.1016/j.jtho.2017.01.005.

17. Y. Kobayashi, Y. Kushihara, N. Saito, S. Yamaguchi, and K. Kakimi, "A Novel Scoring Method. Based on RNA-Seq Immunograms Describing Individual Cancer-Immunity Interactions," *Cancer Science* 111 (2020): 4031–4040, https://doi.org/10.1111/cas.14621.

18. J. L. Ebersole, R. Peyyala, and O. A. Gonzalez, "Biofilm-Induced Profiles of Immune Response Gene Expression by Oral Epithelial Cells," *Molecular Oral Microbiology* 34 (2019): 12251, https://doi.org/10.1111/omi.12251.

19. L. D. Moore, T. Le, and G. Fan, "DNA Methylation and Its Basic Function," *Neuropsychopharmacology* 38 (2013): 23–38, https://doi.org/10.1038/npp.2012.112.

20. J. Reidy, E. McHugh, and L. F. Stassen, "A Review of the Relationship Between Alcohol and Oral Cancer," *Surgeon* 9, no. 5 (2011): 278–283, https://doi.org/10.1016/j.surge.2011.01.010.

21. N. Shah and S. Sukumar, "The *HOX* Genes and Their Roles in Oncogenesis," *Nature Reviews Cancer* 10 (2010): 361–371, https://doi.org/10.1038/nrc2826.

22. Y. Feng, T. Zhang, Y. Wang, et al., "Homeobox Genes in Cancers: From Carcinogenesis to Recent Therapeutic Intervention," *Frontiers in Oncology* 11 (2021): 770428, https://doi.org/10.3389/fonc.2021.770428.

23. K. S. R. Padam, R. Morgan, K. Hunter, S. Chakrabarty, N. A. N. Kumar, and R. Radhakrishnan, "Identification of HOX Signatures Contributing to Oral Cancer Phenotype," *Science Reports* 12 (2022): 10123, https://doi.org/10.1038/s41598-022-14412-6.

24. I. Struzycka, "The Oral Microbiome in Dental Caries," *Polish Journal of Microbiology* 63 (2014): 127–135.

25. M. A. Curtis, P. I. Diaz, and T. E. Van Dyke, "The Role of the Microbiota in Periodontal Disease," *Periodontology 2000* 83 (2020): 14–258, https://doi.org/10.1111/prd.12296.

26. C. M. Healy and G. P. Moran, "The Microbiome and Oral Cancer: More Questions Than Answers," *Oral Oncology* 89 (2019): 30–33, https://doi.org/10.1016/j.oraloncology.2018.12.003.

27. A. C. Tanner, B. J. Paster, S. C. Lu, et al., "Subgingival and Tongue Microbiota During Early Periodontitis," *Journal of Dental Research* 85 (2006): 318–323, https://doi.org/10.1177/154405910608500407.

28. Y. Li, X. Tan, X. Zhao, et al., "Composition and Function of Oral Microbiota Between Gingival Squamous Cell Carcinoma and Periodontitis," *Oral Oncology* 107 (2020): 104710, https://doi.org/10.1016/j.oraloncology.2020.104710.

29. J. P. Lazos, E. D. Piemonte, H. E. Lanfranchi, and M. N. Brunotto, "Characterization of Chronic Mechanical Irritation in Oral Cancer," *International Journal of Dentistry* 7 (2017): 6784526, https://doi.org/10.1155/2017/6784526.

30. C. Li, J. Cui, L. Zou, L. Zhu, and W. Wei, "Bioinformatics Analysis of the Expression of HOXC13 and Its Role in the Prognosis of Breast Cancer," *Oncology Letters* 19 (2020): 899–907, https://doi.org/10.3892/ol.2019.11140.

31. M. Dai, J. Song, L. Wang, K. Zhou, and L. Shu, "HOXC13 Promotes Cervical Cancer Proliferation, Invasion and Warburg Effect Through β-Catenin/c-Myc Signaling Pathway," *Journal of Bioenergetics and Biomembranes* 53 (2021): 597–608, https://doi.org/10.1007/s10863-021-09908-1.

32. H. Li, P. Gao, H. Chen, et al., "HOXC13 Promotes Cell Proliferation, Metastasis and Glycolysis in Breast Cancer by Regulating DNMT3A," *Experimental and Therapeutic Medicine* 26 (2023): 439, https://doi.org/10.3892/etm.2023.12138.

33. W. Li, Q. Zhu, S. Zhang, L. Liu, H. Zhang, and D. Zhu, "HOXC13-AS Accelerates Cell Proliferation and Migration in Oral Squamous Cell Carcinoma via miR-378g/HOXC13 Axis," *Oral Oncology* 111 (2020): 104946, https://doi.org/10.1016/j.oraloncology.2020.104946.

34. J. Smith, S. Sen, R. J. Weeks, M. R. Eccles, and A. Chatterjee, "Promotor DNA Hypermethylation and Paradoxical Gene Activation," *Trends in Cancer* 6 (2020): 392–406, https://doi.org/10.1016/j.trecan.2020.02.007.

35. M. H. McGuire, S. M. Herbrich, S. K. Dasari, et al., "Pan-Cancer Genomic Analysis Links 3'UTR DNA Methylation With Increased Gene Expression in T Cells," *eBioMedicine* 43 (2019): 127–137, https://doi.org/10.1016/j.ebiom.2019.04.045.

36. S. Yao, Z. Huang, C. Wei, et al., "CD79A Work as a Potential Target for the Prognosis of Patients With OSCC: Analysis of Immune Cell Infiltration in Oral Squamous Cell Carcinoma Based on the CIBERSORTx Deconvolution Algorithm," *BMC Oral Health* 23 (2023): 411, https://doi.org/10.1186/s12903-023-02936-w.

Supporting Information

Additional supporting information can be found online in the Supporting Information section. **Figure S1:** Kaplan–Meier curves based on disease-free survival rates for GSCC and TSCC in early-stage (pStage I/II) cases (A) and advanced-stage (pStage III/IV) cases (B). **Figure S2:** Kaplan–Meier curves based on disease-free survival rates for GSCC and TSCC in lymph node metastasis-negative cases (A) and lymph node metastasis-positive cases (B). **Figure S3:** Results of gene expression analysis and enrichment analysis using genes observed in the tumor/normal gene expression ratio in each area. (A, C) Volcano plot indicating gene expression in gingival (A) and tongue (C) tumor/normal gene expression ratios. An absolute value of $|\log FC| > 1$ and $p < 0.05$ were used as cutoffs. (B, D) Characteristic pathways in gingival (B) and tongue (D) tumor/normal gene expression ratios. **Figure S4:** Cutoff value and Kaplan–Meier curve of *HOXC13* expression ratio (tumor/normal) in TSCC cases (A) and cutoff value of *HOXC13* expression ratio (tumor/normal) in GSCC cases (B). **Figure S5:** Slight correlation was observed between methylation and gene expression in the 3′ UTR of *HOXD11*. **Figure S6:** Violin plots comparing 22 types of immune cells between the tumor and normal areas in GSCC cases (A) and TSCC cases (B). **Table S1:** Clinicopathological characteristics of GSCC in clusters 1 and 2 are shown in Figure 3A. **Table S2:** Clinicopathological characteristics of TSCC in clusters 1 and 2 are shown in Figure 3B. **Table S3:** Information on the clinicopathological characteristics of GSCC in *HOXC13* expression ratio (tumor/normal) ≥ 7.0 or < 7.0.